Bull. Mater. Sci. (2018) 41:99
https://doi.org/10.1007/s12034-018-1616-0

Synthesis, characterization and dielectric properties of TiO_2–CeO_2 ceramic nanocomposites at low titania concentration

TOKEER AHMAD[1,*], MOHD SHAHAZAD[1], MOHD UBAIDULLAH[1,2] and JAHANGEER AHMED[2]

[1]Nanochemistry Laboratory, Department of Chemistry, Jamia Millia Islamia, New Delhi 110025, India
[2]Department of Chemistry, College of Science, King Saud University, Riyadh 11451, Saudi Arabia
*Author for correspondence (tahmad3@jmi.ac.in)

MS received 4 September 2017; accepted 25 November 2017; published online 24 July 2018

Abstract. $TiO_{2(x)}$–$CeO_{2(1-x)}$ nanocomposites were prepared at low TiO_2 composition of 5, 10, 15 and 20%, by using TiO_2 and CeO_2 nanoparticles obtained by polymeric citrate precursor method. These nanocomposites were characterized by using powder X-ray diffraction, transmission electron microscopy, scanning electron microscopy, energy dispersive analysis of X-rays and BET surface area studies. BET studies showed the specific surface area of as-prepared nanocomposites in the range of 239–288 $m^2\ g^{-1}$. Twenty percent of TiO_2-based titania–ceria nanocomposites have smallest average particle size of 30 nm and highest surface area of 288 $m^2\ g^{-1}$ among all the as-prepared nanocomposites. The dielectric characteristics were measured as a function of frequency and temperature. The dielectric constant of $TiO_{2(x)}$–$CeO_{2(1-x)}$ at room temperature was 35.6 (maximum) at 500 kHz for $x = 0.20$.

Keywords. Polymeric citrate precursor method; nanocomposites; dielectric properties.

1. Introduction

The worldwide energy demand in electronic devices is growing day by day since the world population is increasing continuously. The portability of such devices is a very important characteristic to utilize them conveniently and efficiently. Therefore, constant efforts were made for miniaturization of the components used to create such devices, which demands the synthesis of novel materials with high dielectric constant, low dielectric loss and high thermal stability [1]. The nanosized titania (TiO_2) owing to its common availability, nontoxicity, high thermal stability and high dielectric constant have attracted considerable attention of material scientists. Although TiO_2 is known to exist mostly in anatase, rutile and brookite crystallographic forms, but anatase and rutile forms are more popular polymorphs of TiO_2. Rutile form was stable at higher temperature as compared to the anatase form of TiO_2 [2]. Nanocrystalline anatase TiO_2 has applications in water purification to remove organic pollutants [3], in light emitting diodes to increase their optoelectronic properties [4] and in biosciences as antibacrial agent [5]. Usually, the rutile form exhibits higher dielectric constant value when compared to the anatase form, hence, it can be used as material in low temperature co-fired ceramics (LTCC) [6]. The difference in crystallographic structure of these two forms is responsible for the high dielectric constant in rutile form. Anatase form consists of a framework of distorted octahedral TiO_6 units sharing four edges, while the rutile form of TiO_2 has chains of trans-edge sharing octahedral TiO_6 units that are connected by sharing corners. A dielectric constant of 80 for rutile TiO_2 nanoparticles was reported in literature [7]. Wypych *et al* [8] have synthesized nanosized TiO_2 by using different chemical methods at different synthesis temperatures for their dielectric characterization. The study revealed that the size of nanoparticles, relative density and synthesis temperature have considerable effect on the dielectric characteristics of TiO_2. TiO_2 nanoparticles synthesized by sol–gel method at 600 and 850°C temperatures were stabilized in anatase and rutile structures, respectively. The room temperature dielectric constants were found to be 18.9 (for anatase) and 63.7 (for rutile) at 1 MHz frequency. Whereas TiO_2 nanoparticles synthesized using Pechini method at 900°C showed mixed forms (anatase and rutile) for which room temperature dielectric constant was 17 due to the presence of anatase phase [8]. Marinel *et al* [9] reported dielectric constant value of about 100 for TiO_2 nanoparticles, sintered at temperature 1000–1300°C. Cubic CeO_2 has fluorite-like structure. The fluorite structure of CeO_2 is stable over the wide range of temperatures with high dielectric constant value ($k = 23$) [10], hence, it is considered as a promising candidate as gate dielectric material in metal oxide semiconductor and memory devices for next-generation devices [11–13].

The composites exhibit the distinct properties different than that of its initial constituent materials due to large interfacial interaction [14,15]. Thus, a series of nanocomposites were synthesized for their structural characterization

and properties, such as TiO_2–SiO_2 [16], ZrO_2–SiO_2 [17–22], CeO_2–ZrO_2 [23–27] and CeO_2–TiO_2 [28–30]. Some triphasic composites viz., CeO_2–ZrO_2–SiO_2 and TiO_2–ZrO_2–SiO_2 were also reported in literature [31–35]. Mostly, TiO_2–CeO_2 ceramic nanocomposite powders and films were investigated for their applications in catalysis [36–40], electrochromic devices [41–46] and oxygen sensors [47].

Numerous chemical methods were reported in literature for the synthesis of various simple and complex metal oxide nanostructures viz., reverse micelles [48], solvothermal [49], hydrothermal [50], polymeric citrate precursor [51] methods, etc. Several methods are also known for the fabrication of TiO_2–CeO_2 nanocomposites, such as sol–gel [52], solvothermal [53], hydrothermal [54,55] and precipitation [56] methods, etc. In this paper, pure TiO_2 and CeO_2 nanoparticles were synthesized by using polymeric citrate precursor method. The synthesis of $TiO_{2(x)}$–$CeO_{2(1-x)}$ (where w/w x is $= 0.05, 0.10, 0.15$ and 0.20) nanocomposites was carried out by using as-prepared TiO_2 and CeO_2 nanoparticles in suitable amounts. The nanocomposites were extensively characterized by powder X-ray diffraction (PXRD), scanning electron microscopy (SEM), transmission electron microscopy (TEM), energy dispersive analysis of X-rays (EDAX) and BET surface area studies. The dielectric characteristics of the nanocomposites were studied as a function of frequency and temperature.

2. Experimental

2.1 *Chemicals required*

The chemicals used were citric acid (SRL, 99.5%), ethylene glycol (SDFCL, 99%), titanium isopropoxide (Sigma-Aldrich, 97%) and cerium chloride heptahydrate (CDH, 99%). All the chemicals were used without any further purification. The double-distilled water was used throughout the synthesis of nanocomposites.

2.2 *Synthesis of precursor nanoparticles*

Twenty-one grams and fourteen milligrams of dry citric acid was added to the beaker containing 1.4 ml of ethylene glycol on constant stirring. 23.6 ml double-distilled water was added to the beaker containing ethylene glycol to obtain a clear solution and stirred for 30 min. The inert chemical setup was designed by continuous purging of nitrogen gas in which 0.74 ml titanium isopropoxide was added to the original solution, so that ethylene glycol, citric acid and titanium isopropoxide were fixed at the molar ratio of 10:40:1. Initially, the white precipitates were obtained due to titanium hydroxide formation, which was dissolved on continuous stirring under nitrogen atmosphere. The stirring was allowed for 3 h at room temperature to form clear transparent solution. The solution was further stirred for 2 h at 55 ± 5°C to increase the viscosity of the solution. The viscous solution was transferred to muffle furnace and heated for 20 h continuously at 135°C temperature, so that the excess of solvent can be removed in the form of vapours and to accelerate the polymerization reaction. The polymeric gel was further worked up at 300°C (2 h) to obtain the black charred product, which was grounded to the fine powder (precursor). The black fine powder was then heated in microprocessor-controlled high-temperature furnace at 500°C for 20 h to obtain anatase form of TiO_2. The fine powder was again annealed at 800°C (10 h) to obtain ultrapure, fine and light-yellowish white powder of rutile TiO_2. The reason to obtain rutile phase is that it has high dielectric constant, which may enhance the dielectric characteristics of nanocomposites.

To prepare CeO_2 nanoparticles, 25 ml of 0.1 M $CeCl_3 \cdot 7H_2O$ was added to the beaker containing 1.4 ml of ethylene glycol with constant stirring. Twenty-one grams and fourteen milligrams of citric acid was added slowly, so that a milky colour was obtained, which disappeared soon into a clear transparent solution and stirred for 3 h at room temperature. The rest of the procedure was same as in the synthesis of TiO_2 nanoparticles.

2.3 *Synthesis of nanocomposites*

TiO_2–CeO_2 nanocomposites were prepared by mixing TiO_2 and CeO_2 using 5, 10, 15 and 20% w/w amounts of TiO_2, followed by proper grinding for 1 h. To increase adhesion of nanopowders, few drops of 5% polyvinyl alcohol (PVA) was added to the mixture, which was allowed for drying at 100°C for 1 h. The powders were then compressed to pellets and sintered at 1000°C for 10 h for composites measurements. Two pellets of each nanocomposite were prepared. One of the pellets was used for dielectric properties measurement and other was grinded for 1 h to obtain fine powder to perform other characterizations.

2.4 *Characterization*

Bruker D8 advanced X-ray diffractometer using Ni-filtered CuKα radiations of wavelength (λ) $= 1.5416$ Å was used for XRD studies. The patterns were recorded in the 2θ range of 20–80° with the step time of 1 s and step size of 0.05°. The lattice parameters were obtained by using the stripping procedure on Kα_2 reflections. SEM studies were carried out to analyse the morphology of the as-prepared samples on FEI SEM (model: Nova Nano SEM 450, Hillsboro, OR). The SEM images were obtained in powder form for the samples, which were obtained by grinding the sintered pellets at various magnifications. The elemental analysis was carried out by EDAX on 127 eV Bruker EDX detector to estimate the composition of the nanocomposites. TEM measurements of the nanocomposites were studied on FEI Technai $G^2$20 TEM at 200 kV accelerating voltage. For the preparation of TEM specimens, a small amount of sample in fine powder form was taken and dispersed in absolute ethanol to be sonicated. The sonication was done for half an hour. A

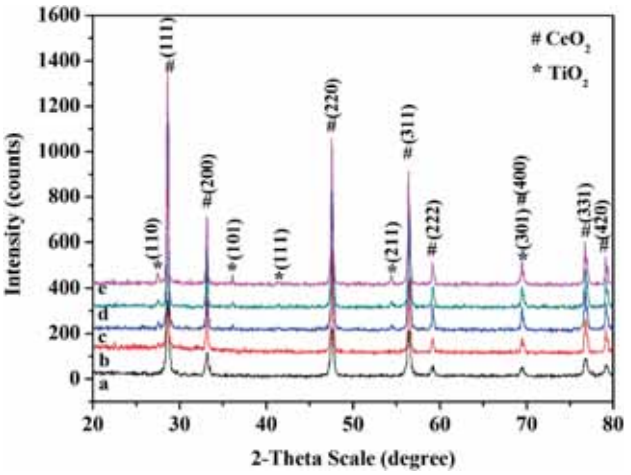

Figure 1. X-ray diffraction patterns of ceria (**a**) and titania–ceria nanocomposites for (**b**) $x = 0.05$, (**c**) $x = 0.10$, (**d**) $x = 0.15$ and (**e**) $x = 0.20$.

drop of the dispersed sample with the help of micropipette (100 µl) was placed on a carbon-coated copper grid and dried at 100°C.

The specific surface areas of as-prepared samples were determined at liquid nitrogen temperature (77 K) using 'multipoint BET method' using BET surface area analyzer (Nova 2000e, Quantachrome Instruments, USA). Fifty milligrams of the sample powder was taken in the sample cell and degassing was done at 250°C for 3 h in vacuum to remove the contaminants, such as gases and water vapours adsorbed by the sample. The degassed sample was then analysed. The sample was taken into a cell and kept at one station. A known amount of the nitrogen gas was admitted into the sample cell acquiring the experimental data. During the adsorption, the pressure changed in the sample cell and finally, the equilibrium has reached. The specific surface area was computed with the help of multipoint BET equation using BET plots. The detailed estimation of specific surface area from the BET curves was reported elsewhere [57]. Dielectric properties of as-synthesized nanocomposites were recorded on HFLCR meter (model: 6505P; Make: Wayne Kerr, UK). Before performing the dielectric measurements, the diameter and thickness of the pellets were measured and area of pellets was calculated to explore the dielectric characteristics of the nanocomposites using the values of capacitance.

3. Results and discussion

The XRD studies of $TiO_{2(x)}$–$CeO_{2(1-x)}$ ($x = 0.05, 0.10, 0.15$ and 0.20) nanocomposites were carried out after sintering the sample pellets at 1000°C for 10 h. PXRD patterns were

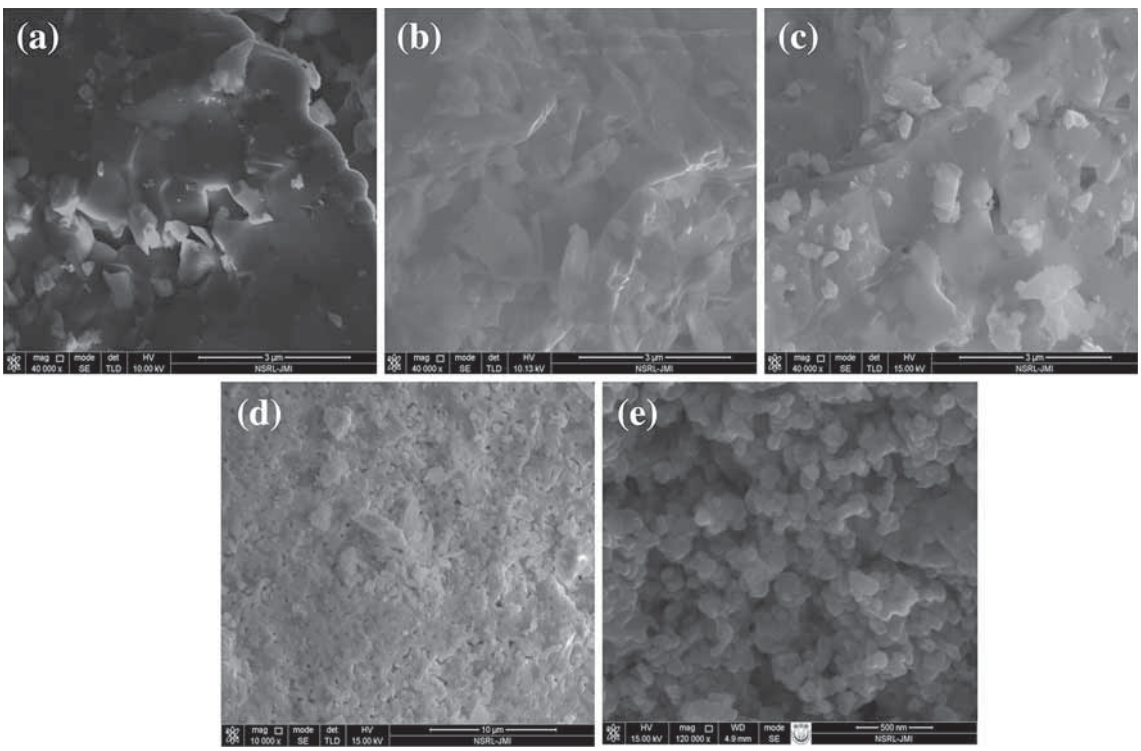

Figure 2. SEM micrographs of titania–ceria nanocomposites for (**a**) $x = 0.05$, (**b**) $x = 0.10$, (**c**) $x = 0.15$, (**d**) $x = 0.20$ and (**e**) pure ceria nanoparticles.

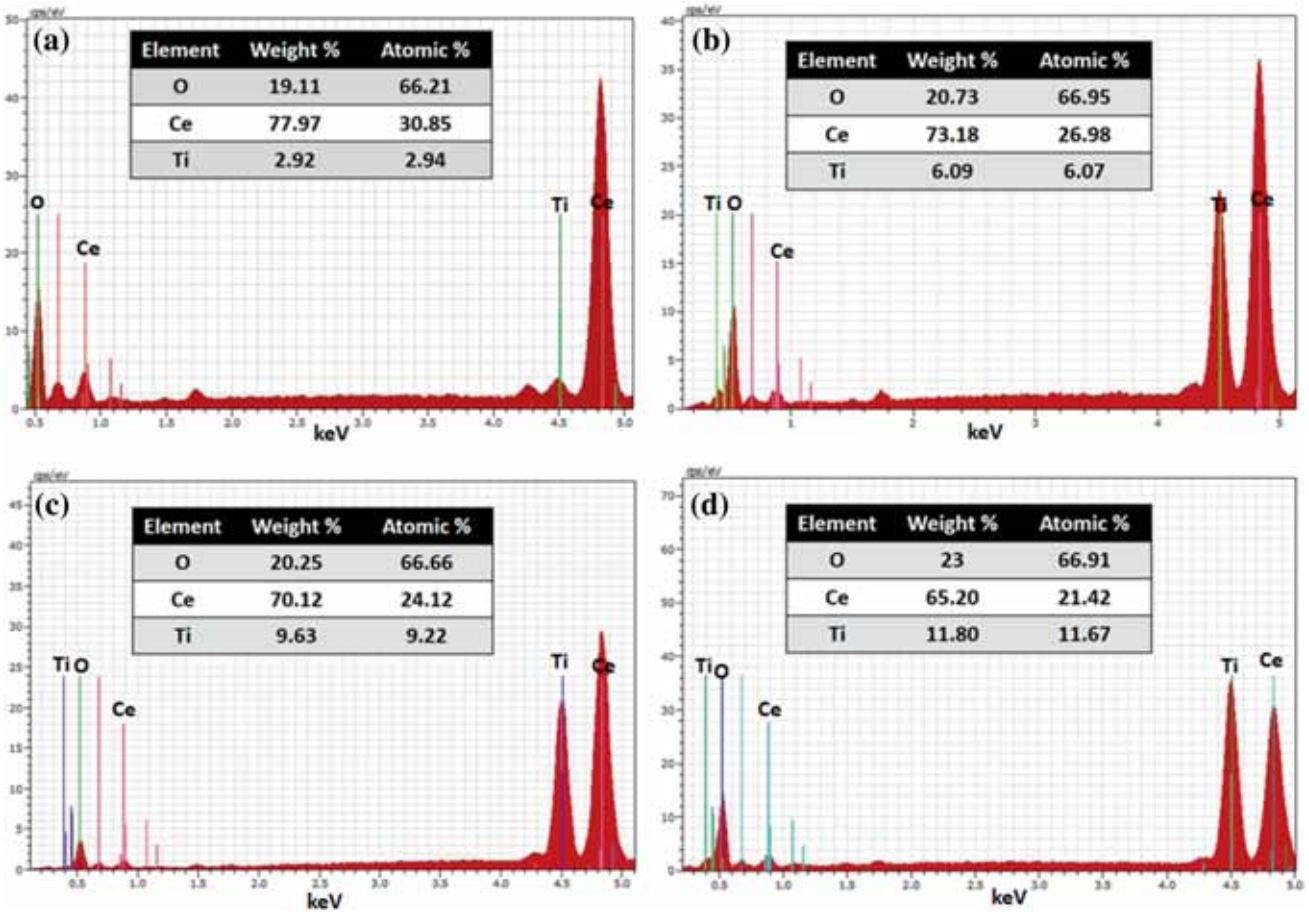

Figure 3. EDAX spectra of titania–ceria nanocomposites for (**a**) $x = 0.05$, (**b**) $x = 0.10$, (**c**) $x = 0.15$ and (**d**) $x = 0.20$.

satisfactorily indexed to the CeO_2 cubic structure (JCPDS no. 81-0792) (space group Fm3m (225) and $a = 5.412$ Å) and tetragonal (rutile) structure (JCPDS no. 83-2242) (space group $P4_2/mnm$ (136), $a = 4.59$ and $b = 2.96$ Å) (figure 1). All the samples were biphasic and highly crystalline in nature. It is clearly seen from the XRD studies that there is no peak other than CeO_2 and TiO_2, which confirm that as-prepared materials were TiO_2–CeO_2 nanocomposites. The presence of (110), (101), (111), (211) and (301) peaks at 2θ values of 27.5, 36, 41, 54.3 and 69.5°, respectively, confirm the presence of rutile TiO_2. Finally, PXRD data revealed that peak intensity of rutile TiO_2 phase increased with increase in the composition of TiO_2 in host CeO_2 matrix.

The morphology and texture of $TiO_{2(x)}$–$CeO_{2(1-x)}$ nanocomposites were investigated by using SEM studies as shown in figure 2a–d. The SEM images clearly show the biphasic morphology, in which TiO_2 nanoparticles could be seen distinctly over CeO_2 rough surface. The SEM images of pure CeO_2 nanoparticles showed that the nanoparticles were agglomerated acquiring nearly spherical shapes as shown in figure 2e. This is visible from figure 2d with increased w/w% composition of titania, the nanocomposites showed increased density and hence, dense surface could be seen. The EDAX studies showed that the loaded compositions of the precursor nanoparticles have close agreement with the calculated composition of nanocomposites as shown in figure 3a–d. XRD and EDAX studies corroborate to the formation of TiO_2–CeO_2 nanocomposites.

The particle size and size distribution of titania–ceria nanocomposites were estimated by TEM study as shown in figure 4a–d. The particles were nearly hexagonal, and some of them were found spherical with reasonable agglomeration. The average particle size of nanocomposites was in the range of 30–46 nm. The significant decrease in average particle size was observed with increase in composition of TiO_2. The smallest particle size of 30 nm was observed by TEM for 20% TiO_2-based composites, which was in good agreement with the size of pure CeO_2 particles. Figures 2e and 4e show that the SEM and TEM images of pure CeO_2 nanoparticles have 100% ceria, which is agglomerated and larger in size as compared to nanocomposites in which less ceria is present. The observed decrease in average particle size from 46 to 30 nm with increase in composition of TiO_2 is associated with the

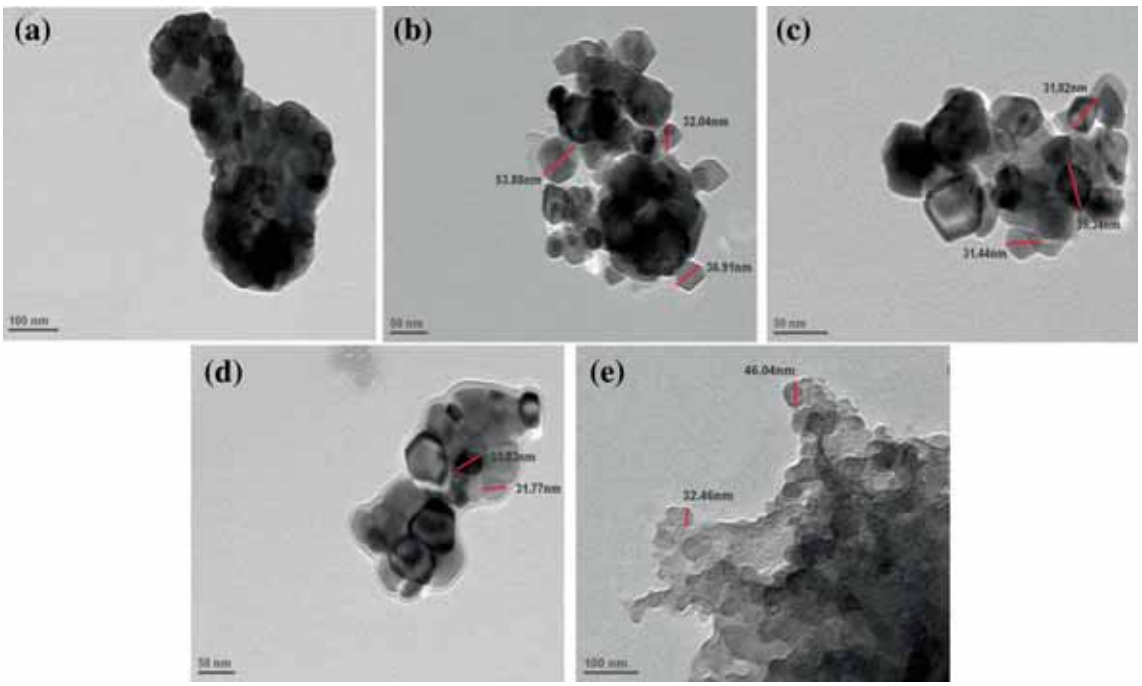

Figure 4. TEM images of titania–ceria nanocomposites for (**a**) $x = 0.05$, (**b**) $x = 0.10$, (**c**) $x = 0.15$, (**d**) $x = 0.20$ and (**e**) pure ceria nanoparticles.

better microstructural formation for increased composition of titania.

The surface area studies of as-prepared nanocomposites were carried out in the P/P_0 range of 0.05–0.35 using multipoint BET equation as shown in figure 5. The BET plots revealed that the specific surface area of the nanocomposites was found in the range of 239–288 $m^2\ g^{-1}$. The specific surface area of pure CeO_2 was found to be 258 $m^2\ g^{-1}$. An increase in the surface area is observed with increase in the percent composition of TiO_2 in nanocomposites. The particle size was also estimated by using equation $D_{BET} = 6000/(\rho * S_w)$. In this equation, D_{BET} represents the average particle size in nm, ρ represents theoretical density in g cm^{-3} and S_w represents specific surface area in $m^2\ g^{-1}$ [57,58]. The particle size using above BET studies was found to be 7.4, 7.1, 6.9 and 5.9 nm for the TiO_2–CeO_2 nanocomposites with 5, 10, 15 and 20% TiO_2 concentrations, respectively. The grain size values were smaller as compared to TEM sizes, because BET size theory applies for the spherical particles with smooth surface. Therefore, the BET size results are qualitatively correct, however, in the present studies, the particles do not have spherical geometry and smooth surface and hence, the shape factor was considered for nonspherical nanoparticles [59].

The dielectric properties of as-prepared ceramic nanocomposites were studied as a function of frequency and temperature after sintering the pellets at 1000°C for 10 h. The dielectric characteristics (dielectric constant and loss

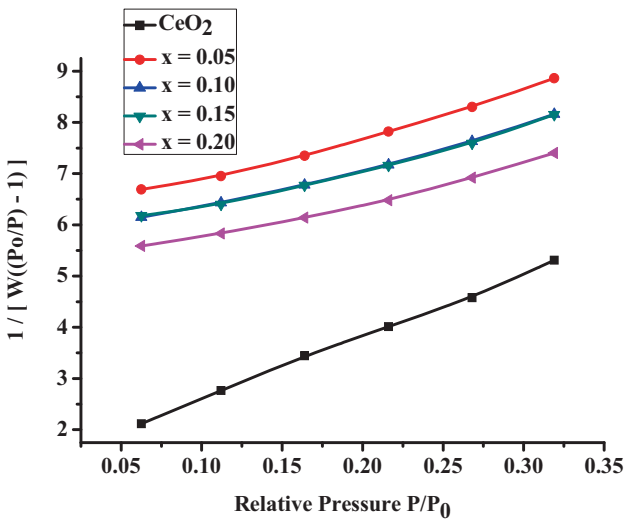

Figure 5. BET surface area plots of titania–ceria nanocomposites for (a) $x = 0.05$, (b) $x = 0.10$, (c) $x = 0.15$, (d) $x = 0.20$ and (e) pure ceria nanoparticles.

factor) were determined with the variation of frequency in a range from 20 kHz to 1 MHz at room temperature as shown in figure 6a–d. The room temperature dielectric constant and dielectric loss values were found to be 27, 0.0064 (for $x = 0.05$), 32.8, 0.0079 (for $x = 0.10$), 34.8,

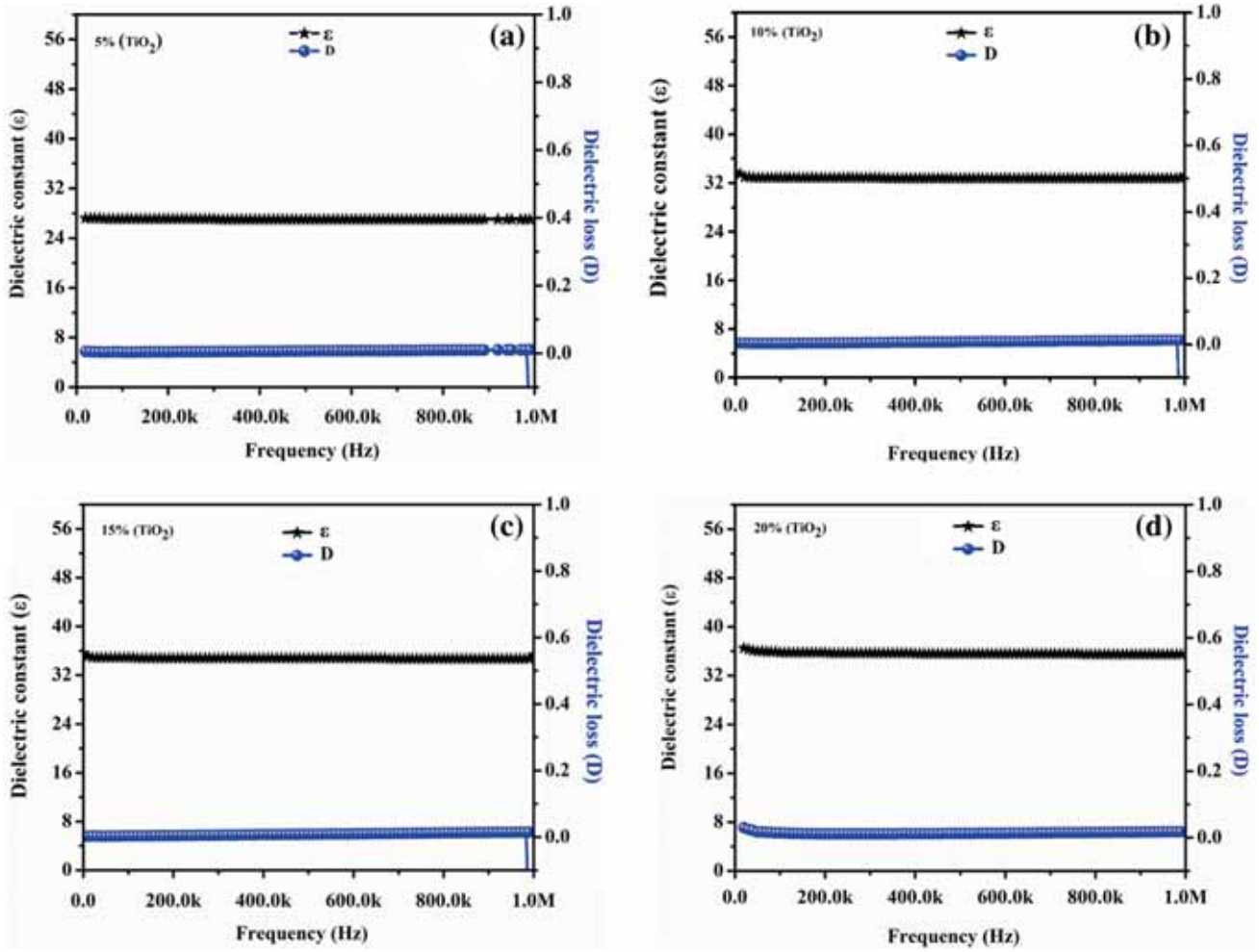

Figure 6. The variations of dielectric constant and dielectric loss with frequency at room temperature of titania–ceria nanocomposites for (**a**) $x = 0.05$, (**b**) $x = 0.10$, (**c**) $x = 0.15$ and (**d**) $x = 0.20$.

0.0079 (for $x = 0.15$) and 35.6, 0.0125 (for $x = 0.20$), respectively, for $TiO_{2(x)}$–$CeO_{2(1-x)}$ nanocomposites at 500 kHz. Comparatively, high dielectric constant of nanocomposites may be associated with the inhomogeneous structure, which may cause higher space charge polarization leading to higher dielectric constant. The increase in dielectric constant from 27 to 35.6 with increase in %composition of titania is attributed to increase in surface area and decrease in particle size of nanocomposites. The number of dipoles increases at surfaces with decrease in particle size, which contributes to the high degree of polarization and the charges move within the grains that piled up at grain boundaries [60]. The dielectric characteristics were found to be stable with frequency for $TiO_{2(x)}$–$CeO_{2(1-x)}$ ($x = 0.05, 0.10, 0.15$ and 0.20) ceramic nanocomposites, which might be associated with the failure of electric dipoles, which follow up the fast variation of alternating applied field [61].

The dielectric constant and dielectric loss of as-prepared nanocomposites were also studied as a function of temperature at 500 kHz as shown in figure 7a–d. The experimental values of dielectric constant and dielectric loss for all ceramic nanocomposites ($TiO_{2(x)}$–$CeO_{2(1-x)}$ ($x = 0.05, 0.10, 0.15$ and 0.20)) were found to be stable up to 250°C and thereafter, an increment with temperature was observed. The increase of dielectric constant beyond 250°C may be due to the increased polarization with the applied field, which cause an interaction between the field and the dielectric polarization with temperature [62]. The dielectric characteristics were found to be 27.3, 0.025 (for $x = 0.05$), 33, 0.033 (for $x = 0.10$), 34.7, 0.041 (for $x = 0.15$) and 35.4, 0.042 (for $x = 0.20$) for dielectric constant and dielectric loss, respectively, for $TiO_{2(x)}$–$CeO_{2(1-x)}$ nanocomposites at 200°C. The dielectric constant was found to increase with increase of %composition of TiO_2 in TiO_2–CeO_2 nanocomposites as shown in figure 8,

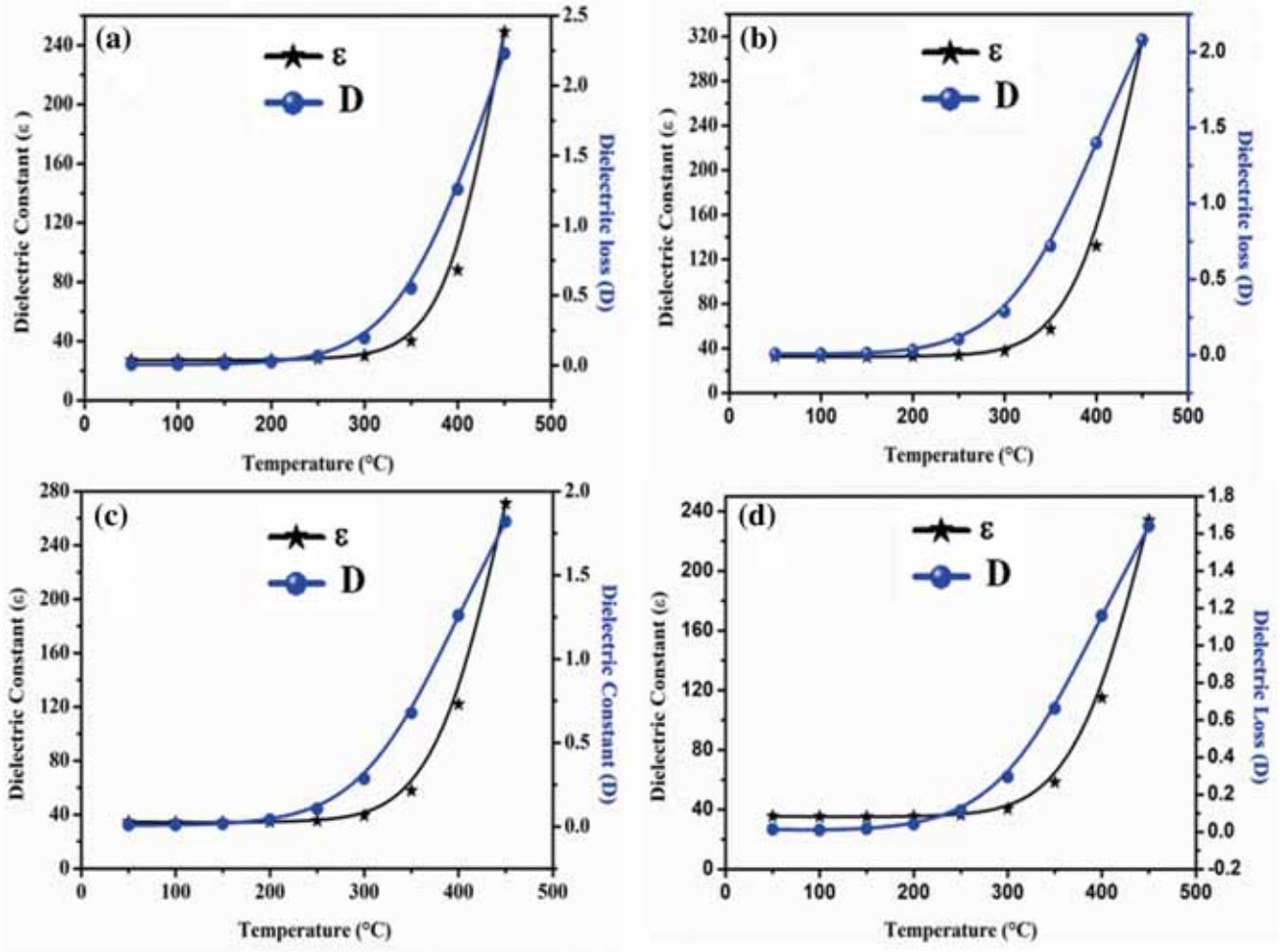

Figure 7. The variations of dielectric constant and dielectric loss with temperature at 500 kHz frequency of titania–ceria nanocomposites for (**a**) $x = 0.05$, (b) $x = 0.10$, (**c**) $x = 0.15$ and (**d**) $x = 0.20$.

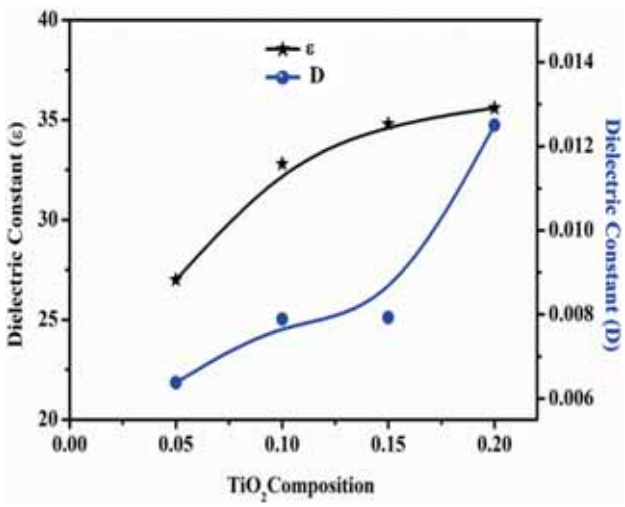

Figure 8. The variations of dielectric constant and dielectric loss with TiO_2 composition of titania–ceria nanocomposites at room temperature and 500 kHz frequency.

which may be associated with high dielectric constant of TiO_2 nanoparticles.

4. Conclusions

Ceramic nanocomposites of $TiO_{2(x)}$–$CeO_{2(1-x)}$ ($x = 0.05$, 0.10, 0.15 and 0.20) were successfully synthesized by using appropriate amounts of TiO_2 and CeO_2 nanoparticles, which were prepared by polymeric citrate precursor route. As-prepared nanocomposites were biphasic with reasonable agglomeration and rough surfaces. The nanocomposites were nearly hexagonal along with some spherical particles. The particle sizes decrease from 46 to 30 nm on increasing the titania weight% concentration from 5 to 20%. As a result, the specific surface area increases significantly with increase in %composition of titania. The nanocomposites exhibit high stability of dielectric properties with variation of frequency from 20 to 500 kHz as well as with variation of temperature up

to 250°C. The dielectric constant was found to increase with increase in %composition of TiO_2 in TiO_2–CeO_2 nanocomposites due to high dielectric characteristics of titania.

Acknowledgements

TA thanks CSIR, Govt. of India, for financial support of the research Project (No. 01(2897)/17/EMR-II). We thank CIF, Jamia Millia Islamia for XRD studies, and AIIMS, New Delhi, for TEM studies. MS thanks to UGC for providing fellowship.

References

[1] Wilk G D, Wallace R M and Anthony J M 2001 *J. Appl. Phys.* **89** 5243
[2] Zhang H and Banfield J F 2002 *Chem. Mater.* **14** 4145
[3] Tayade R J, Surolia P K, Kulkarni R G and Jasra R V 2007 *Sci. Technol. Adv. Mater.* **8** 455
[4] Al-Asbahi B A, Jumali M H H, Yap C C and Salleh M M 2013 *J. Nanomater.* **561534** 1
[5] Ahmad R, Mohsin M, Ahmad T and Sardar M 2015 *J. Hazard. Mater.* **283** 171
[6] Pang L X, Wang H, Zhou D and Yao X 2010 *J. Mater. Sci.* **21** 1285
[7] Nalwa H 1999 (London, UK: Academic Press)
[8] Wypych A, Bobowska I, Tracz M, Opasinska A, Kadlubowski S, Krzywania-Kaliszewska A *et al* 2014 *J. Nanomater.* **124814** 1
[9] Marinel S, Choi D H, Heuguet R, Agrawal D and Lanagan M 2013 *Ceram. Int.* **39** 299
[10] Chiu F C and Lai C M 2010 *J. Phys. D: Appl. Phys.* **43** (075104) 1
[11] Tarnuzzer R W, Colon J, Patil S and Seal S 2005 *Nano Lett.* **5** 2573
[12] Aspinall H C, Bacsa J, Jones A C and Wrench J S 2011 *Inorg. Chem.* **50** 11644
[13] Phokha S, Pinitsoontorn S, Chirawatkul P, Poo-Arporn Y and Maensiri S 2012 *Nanoscale Res. Lett.* **7** 1
[14] Camargo P H C, Satyanarayana K G and Wypych F 2009 *Mater. Res.* **12** 1
[15] Shanker V, Ahmad T and Ganguli A K 2006 *J. Mater. Res.* **21** 816
[16] Nilchi A, Darzi S J, Mahjoub A R and Garmarodi S R 2010 *Colloids Surf. A: Physicochem. Eng. Aspects* **361** 25
[17] Jongsomjit B, Kittiruangrayub S and Praserthdam P 2007 *Mater. Chem. Phys.* **105** 14
[18] Rahulan K M, Vinitha G, Stephen L D and Kanakam C C 2013 *Ceram. Int.* **39** 5281
[19] Gao X, Fierro J L G and Wachs I E 1999 *Langmuir* **15** 3169
[20] Morks M F and Kobayashi A 2008 *J. Mech. Behav. Biomed. Mater.* **1** 165
[21] Sulim I Y, Borysenko M V, Korduban O M and Gun'ko V M 2009 *Appl. Surf. Sci.* **255** 7818
[22] Gun'ko V M, Sulym I Y, Borysenko M V and Turov V V 2013 *Colloids Surf. A: Physicochem. Eng. Aspects* **426** 47
[23] Truffault L, Magnani M, Hammer P, Santilli C V and Pulcinelli S H 2015 *Colloids Surf. A: Physicochem. Eng. Aspects* **471** 73
[24] Reddy B M and Khan A 2005 *Catal. Surv. Asia* **9** 155
[25] Trovarelli A, Boaro M, Rocchini E, Leitenburg C and Dolcetti G 2001 *J. Alloys Compd.* **323–324** 584
[26] Garciia M F, Arias A M, Juez A I, Belver C, Hungriia A B, Conesa J C *et al* 2000 *J. Catal.* **194** 385
[27] Vaidya S, Ahmad T, Agarwal S and Ganguli A K 2007 *J. Am. Ceram. Soc.* **90** 863
[28] Fang J, Bao H, He B, Wang F, Si D, Jiang Z *et al* 2007 *J. Phys. Chem. C* **111** 19078
[29] Jiang B, Zhang S, Guo X, Jin B and Tian Y 2009 *Appl. Surf. Sci.* **255** 5975
[30] Rao K N, Reddy B M and Park S 2010 *Appl. Catal. B* **100** 472
[31] Reddy B M, Thrimurthulu G, Saikia P and Bharali P 2007 *J. Mol. Catal. A: Chem.* **275** 167
[32] Reddy B M, Saikia P, Bharali P, Katta L and Thrimurthulu G 2009 *Catal. Today* **141** 109
[33] Gao J, Guo J, Liang D, Hou Z, Fei J and Zheng X 2008 *Int. J. Hydrogen Energy* **33** 5493
[34] Kim K D and Kim H T 2005 *Colloids Surf. A: Physicochem. Eng. Aspects* **255** 131
[35] Gunawidjaja P N, Holland M A, Mountjoy G, Pickup D M, Newport R J and Smith M E 2003 *Solid State Nucl. Magn. Reson.* **23** 88
[36] Pavasupree S, Suzuki Y, Art S P and Yoshikawa S 2005 *J. Solid State Chem.* **178** 128
[37] Rynkowski J, Farbotko J, Touroude R and Hilaire L 2000 *Appl. Catal. A: Gen.* **203** 335
[38] Yang S, Zhu W, Jiang Z, Chen X and Wang J 2006 *Appl. Surf. Sci.* **252** 8499
[39] Liu Z, Guo B, Hong L and Jiang H 2005 *J. Phys. Chem. Solids* **66** 161
[40] Periyat P, Baiju K V, Mukundan P, Pillai P K and Warrier K G K 2007 *J. Sol-Gel Sci. Technol.* **43** 299
[41] Avellaneda C O, Bulhoes L O S and Pawlika A 2005 *Thin Solid Films* **471** 100
[42] Verma A, Samanta S B, Bakhshi A K and Agnihotry S A 2004 *Solid State Ionics* **171** 81
[43] Sun D L, Heusing S, Puetz J and Aegerter M A 2003 *Solid State Ionics* **165** 181
[44] Ghodsi F E, Tepehan F Z and Tepehan G G 1999 *Electrochim. Acta* **44** 3127
[45] Avellaneda C O and Pawlika A 1998 *Thin Solid Films* **335** 245
[46] Keomany D, Petit J P and Deroo D 1995 *Sol. Energ. Mater. Sol. C* **36** 397
[47] Trinchi A, Li Y X, Wlodarsky W, Kaciulis S, Pandolfi L, Viticoli S *et al* 2003 *Sensor Actuat. B-Chem. B* **95** 145
[48] Ahmad T and Ganguli A K 2004 *J. Mater. Res.* **19** 2905
[49] Ahmad T, Khatoon S, Coolahan K and Lofland S E 2013 *J. Alloys Compd.* **558** 117
[50] Ahmad T and Phul R 2015 *Solid State Phenomena* **232** 111
[51] Ahmad T, Lone I H, Ansari S G, Ahmed J, Ahamad T and Alshehri S M 2017 *Mater. Des.* **126** 331
[52] Magesh G, Viswanathan B, Viswanath R P and Varadarajan T K 2009 *Indian J. Chem. A* **48** 480
[53] Xie J, Jiang D, Chen M, Li D, Zhu J, Lu X *et al* 2010 *Colloids Surf. A* **372** 107
[54] Tong T, Zhang J, Tian B, Chen F, He D and Anpo M 2007 *J. Colloid Interface Sci.* **315** 382

[55] Liu Y, Fang P, Cheng Y, Gao Y, Chen F, Liu Z *et al* 2013 *Chem. Eng. J.* **219** 478
[56] Stengl V, Bakardjieva S and Murafa N 2009 *Mater. Chem. Phys.* **114** 217
[57] Wani I A, Khatoon S, Ganguly A, Ahmed J, Ganguli A K and Ahmad T 2010 *Mater. Res. Bull.* **45** 1033
[58] Li J G, Ikegami T, Wang Y and Mori T 2003 *J. Am. Ceram. Soc.* **86** 915
[59] Waseda Y and Muramastu A 2004 *Springer* (*ISBN* 978-3-662-08863-0) 6
[60] Azam A, Ahmad A S, Chaman M and Naqvi A H 2010 *J. Appl. Phys.* **108** (094329) 1
[61] Bammannavar B K, Naik L R and Chougule B K 2008 *J. Appl. Phys.* **104** (064123) 1
[62] Zamiril R, Ahangar H A, Kaushal A, Zakaria A, Zamiri1 G, Tobaldi D *et al* 2015 *PLoS One* **10** 1